

**Automated daily process for global ionospheric total electron content maps
and satellite ocean altimeter ionospheric calibration based on Global
Positioning System data**

B.A. Iijima, I.L. Harris, C.M. Ho, U.J. Lindqwister, A.J. Mannucci, X. Pi, M.J. Reyes,
L.C. Sparks, B.D. Wilson

Jet Propulsion Laboratory, California Institute of Technology, Pasadena, CA 91109, USA

JASTP manuscript number JASTP.NA.9906

Contact information:

Corresponding author, B.A. Iijima

Tel.: 001 818 354 8503; fax: 001 818 393 5115; e-mail: Byron.A.Iijima@jpl.nasa.gov

All authors are at same address:

Dr. Byron A. Iijima

Jet Propulsion Laboratory, M/S 138-308

4800 Oak Grove Drive

Pasadena, CA 91109

USA

Keywords

Ionosphere, Ocean altimetry, Global Positioning System

Abstract

The accuracy of single-frequency ocean altimeters benefits from calibration of the total electron content (TEC) of the ionosphere below the satellite. Data from a global network of GPS receivers provides timely, continuous, and globally well-distributed measurements of ionospheric electron content. For several months we have been running a daily automatic Global Ionospheric Map process which inputs global GPS data and climatological ionosphere data into a Kalman filter, and produces global ionospheric TEC maps and ocean altimeter calibration data within 24 hours of the end-of-day. Other groups have successfully applied this output to altimeter data from the GFO satellite and in orbit determination for the TOPEX/Poseidon satellite. Daily comparison of the global TEC maps with independent TEC data from the TOPEX altimeter is performed as a check on the calibration whenever the TOPEX data are available. Comparisons of the global TEC maps against TOPEX data will be discussed. Accuracy is best at mid-to-high absolute latitudes ($|\text{latitude}| > 30$ degrees) due to the better geographic distribution of GPS receivers and the relative simplicity of the ionosphere. Our highly data-driven technique is relatively less accurate at low latitudes and especially during ionospheric storm periods, due to the relative scarcity of GPS receivers and the structure and volatility of the ionosphere. However, it is still significantly more accurate than climatological models.

1. Introduction

The Global Positioning System (GPS) maintains a constellation of 27 GPS satellites orbiting at an altitude of 20200 km in three orbital planes. These satellites continuously transmit ranging signals at two frequencies, L1 (1575.42 MHz) and L2 (1221.6 MHz). The International GPS Service (IGS, a consortium of government and academic institutions (Zumberge et al 1994)) and other organizations maintain networks of ground-based GPS receivers, each receiver typically continuously tracking between 4 and 12 GPS satellites at a given time. This tracking data is transmitted back to the operating

institutions, and is typically available within 24 hours from the IGS Data Centers. The IGS network alone has over 200 GPS receivers which have a good global distribution (Fig. 1). This data is excellent for monitoring global and regional ground movement, earth orientation, and tropospheric and ionospheric properties. In particular for this paper, the dual-frequency nature of the GPS signal allows one to extract ionospheric total electron content (TEC, i.e. integrated free electron density) information along the line-of-sight between the satellite and receiver (Lanyi et al 1988). Thus GPS data provide continuous globally well-distributed ionospheric TEC data available in a timely fashion. This data is currently being used at Jet Propulsion Laboratory to produce regional and global maps of ionospheric electron content (Lanyi et al 1988, Wilson et al 1995, Mannucci et al 1998).

Spacecraft which rely on single-frequency ranging through the ionosphere benefit from ionospheric calibrations to remove the effect of ionospheric delay on the range measurements. In particular for this paper, satellite-based ocean altimeters using single-frequency radar altimetry (such as Geosat Follow-On (GFO) and the European Remote Sensing Satellite II (ERS-2)) benefit from calibration of the ionospheric vertical TEC below the satellite. The global GPS data set is very well suited for providing timely ionospheric calibrations. GPS data-based TEC maps have been shown (Yuan et al 1995) to be much more accurate than TEC derived from climatological models such as the International Reference Ionosphere 1995 (IRI-95) (Bilitza et al 1988, Bilitza et al 1998) and the Bent model (Llewellyn et al 1973). (See also the comparisons in Section 4.) In addition, a recent comparison (Komjathy 1999) indicates that the JPL's GPS-based Global Ionosphere Map (GIM) algorithm may be more accurate than other GPS data-dependent ionospheric algorithms for ocean altimetry applications.

We have created an automated system to run the JPL GIM algorithm daily to produce a sub-hourly time-series of global ionospheric vertical TEC maps and altimeter calibration files for GFO and ERS-2 which are being delivered to the U.S. Naval Oceanographic Office. This system is continuously being improved, and this paper

describes the current status of this system, its performance thus far, and planned improvements. Section 2 briefly describes the algorithm. Section 3 describes the system used in the daily automated process. Section 4 describes the accuracy performance of the system as indicated by comparison with data from the TOPEX/Poseidon ocean altimetry satellite. Recent accuracy problems associated with a loss of GPS data due to receiver problems are discussed, as well as possible solutions to the problem. Section 5 discusses the generation of altimeter ionospheric calibration data. Section 6 discusses changes in GIM currently under development.

2. GIM algorithm

The GIM algorithm inputs GPS tracking data from the global network of GPS receivers and produces a quarter-hourly time series of global maps of ionospheric vertical TEC. The following is a brief description of the GIM algorithm being used. For a more complete description see Mannucci et al 1998.

GIM uses the dual-frequency nature of the GPS signal to obtain ionospheric TEC information. The global GPS receivers continuously track the ranging signals broadcast by the GPS satellites at the L1 and L2 frequencies to measure pseudorange (biased range) observables, called P1 and P2, and carrier phase range observables, called L1 and L2. Both the differenced pseudorange, $P2 - P1$, and the differenced carrier phase, $L1 - L2$, contain TEC information. Aside from hardware biases intrinsic to the GPS satellites and receivers, the $P2 - P1$ observable is proportional to the line-of-sight or “slant” TEC between the receiver and satellite. Specifically we define the PI observable,

$$PI = (P2 - P1) / (0.105 \text{ m / TECU}) = B_r + B_s + STEC$$

where B_r and B_s are the receiver and satellite hardware biases respectively, and $STEC$ is the slant TEC between the receiver and satellite. The units used for TEC are TECU where $1 \text{ TECU} = 10^{16} \text{ electrons} / \text{m}^2$. The receiver and satellite hardware biases are caused by the differences between the L1 and L2 group delays associated with the electronics and antennas of the GPS receivers and GPS satellites. This bias is different for each satellite and receiver, and can be quite large--60 TECU biases have been observed in some receivers--and the effect of the bias must be removed to perform accurate ionospheric calibration. However the value of the bias is typically quite stable for a given satellite or receiver from day to day (Sardon et al 1997; Wilson et al 1994; Coco et al 1991). We use the Kalman filter to simultaneously solve for the values of the hardware biases and the ionospheric vertical TEC maps from the GPS data. The carrier phase LI observable

$$LI = (L1 - L2) / (0.105 \text{ m} / \text{TECU}) = STEC + (\text{phase bias})$$

is very similar to the PI observable but has the advantage of much less scatter and the disadvantage of an arbitrary bias due to the cycle ambiguity in the phase. GIM combines unambiguous PI with the smooth LI to produce a smoothed PI data type which is the primary measurement input to the Kalman filter.

Kalman filtering (Bierman 1977, Lichten 1990) is a technique which produces a least-squares fit solution for physical models involving stochastic processes. The Kalman filter is a flexible technique for sensible combination of various data types such as GPS data, climatological model data, and data from other satellites, such as TOPEX altimeter TEC data, DORIS TEC data, and GPS flight receiver occultation data. We currently use GPS smoothed PI data and TEC gradient information derived from a climatological model, and plan to add TOPEX altimeter data and a single-frequency GPS data type which will be described in Sec. 4.

A simple ionospheric model is currently being used in the filter: the ionosphere is modeled as a thin shell at 450 km. The slant TEC data are converted to vertical using an obliquity function, $M(E)$, dependent only on the local elevation angle of the satellite relative to the receiver. The line-of-sight vector pierces the thin shell at a "pierce point". The vertical TEC dependence on latitude and longitude is parametrized as a linear combination of basis functions $b_i(\lambda, \phi)$ with coefficients c_i where λ and ϕ are the solar-magnetic latitude and longitude respectively. (The solar-magnetic frame is the frame specified by a z axis in the direction of the geomagnetic dipole axis, and the zero longitude meridian defined by the position of the sun. The reason for using this frame is explained below.) Mathematically the model of the GPS PI observables can be expressed as

$$PI = B_r + B_s + M(E) \sum_i c_i b_i(\lambda, \phi)$$

where λ, ϕ is the pierce point. Using the smoothed PI data, the Kalman filter simultaneously solves for the hardware biases and the coefficients c_i . The dominant drivers of the horizontal distribution of ionospheric electron content are the ionization of the atmosphere by the sun and the dynamic effects of the earth's magnetic field, so that the horizontal distribution of electron content is more stationary in the solar-magnetic frame than in other frames. The coefficients c_i are permitted to vary in time as a random walk stochastic process. TEC gradient data from IRI-95 or Bent climatological model are also added to the Kalman filter to help fill gaps in GPS data coverage. These last two features each aid in filling spatial/temporal gaps in GPS data coverage, and effect a spatial/temporal interpolation which is most reliable under non-storm conditions.

The basis functions currently being used are locally (rather than globally) supported basis functions based on a bicubic spline technique developed at JPL (Lawson 1984).

The ionospheric shell height and obliquity function were selected by examining global TEC map agreement with TEC data from the TOPEX/Poseidon satellite and analyzing the repeatability of daily hardware bias solutions (Yuan et al 1995). This study led to the use of an ionospheric shell at 450 km to compute line-of-sight shell pierce points, and an obliquity function based roughly on a thick shell between 450 and 650 km. (For more details see Mannucci et al 1998.) This simple thin/thick shell approach is subject to modeling errors, especially at low elevations and low latitudes where the horizontal/vertical structure is quite complex. (Vladimer et al, 1997) However, removing too much low elevation GPS data from GIM processing compromises the spatial/temporal sampling of the ionosphere required by GIM. We have chosen to use an elevation cutoff of 10 degrees in our data processing. The low elevation modeling error is mitigated in part by the combination of high and low elevation data in our solutions. We are working to improve our three-dimensional modeling of the ionosphere.

Fig. 2 shows a typical GIM TEC map. (The data shown are for 18 UT on 6 July 1998. GIM results for this data will be discussed further in Sec. 4.) It shows the features typical of ionospheric TEC, such as the equatorial peak structure slightly after local noon near the geomagnetic equator. Also shown are the 98 GPS receivers used in the solution for this day. Although more GPS receivers are available, they do not add significantly to the geographic coverage, while adding significantly to computation time. Also, since we use the GIM process to extract both the ionosphere map and GPS receiver and satellite hardware biases from the GPS data, we have also included GPS receivers in the processing whose biases are required for other purposes although they may not significantly contribute to geographic coverage (especially in California).

3. Daily GIM process

We are currently running GIM daily in a completely automated process, generating global vertical TEC maps and ocean altimeter calibrations for the GFO and ERS-2 satellites and delivering them to the U.S. Naval Oceanographic Office. Two similar products are generated daily: A quick-look product which is required to be delivered within 24 hours of the end of day; and a final product produced within 72 hours of the end of day which has the advantage of additional GPS data available after the quick-look solution is computed. Because of the timeliness requirements on the products, system robustness is a primary concern in the design.

Fig. 3 shows the data flow of the automated calibration process. The entire system runs on a single HP 9000/780 platform. GPS data are imported from the JPL GPS Data Handling Facility and the IGS Data Centers. From the many stations available, 80 to 98 are selected to optimize geographic coverage. The GPS data are then edited and Kalman filtered to produce a quarter-hourly time series of global ionospheric vertical TEC maps. The previous day's final solution is used as a priori data to initialize the Kalman filter.

TOPEX data (see Sec. 4) are imported if available, and a comparison between the TOPEX TEC data and GIM maps is performed to validate the maps. If TOPEX data are not available, a comparison is performed between the GIM maps and the IRI-95 climatological model as a rough quality check on the GIM products before delivery.

The ERS-2 and GFO ephemerides are imported. The GIM TEC values are evaluated along the altimeter ground tracks, and the super-satellite TEC is removed as described in Section 5. IONEX (Schaer et al 1998) format vertical TEC map files (which also include L1/L2 bias solutions) are also generated for submission to the IGS. If the GIM maps pass the quality check based on TOPEX and/or climatological comparison, then the altimeter calibration and IONEX files are exported.

The system places plots of TOPEX comparisons and postfit residuals onto an internal web site for operators to inspect. A completely redundant process is run on a second platform to ensure system reliability.

We have been generating GIM solutions daily within 24 hours for several months. The GFO altimeter calibrations have been applied successfully to GFO altimeter data (Lillibridge 1998). The GIM global maps as well as GIM L1/L2 satellite biases are also being used with success to calibrate single-frequency data from the GPS receiver on board the TOPEX/Poseidon satellite which is used in TOPEX/Poseidon orbit determination (Lough et al 1998).

4. Comparisons of GIM TEC with TOPEX TEC data

The TOPEX/Poseidon ocean altimetry satellite orbits at an altitude of 1336 km with an orbital period of 112 minutes and an inclination of 66 degrees, providing good coverage of the Earth's oceans each day. Its orbital plane rotates in the solar frame about once every 120 days. TOPEX/Poseidon carries the dual-frequency TOPEX radar altimeter which enables it to measure the vertical TEC below it and self-calibrate the ionospheric delay in its radar altimetry data. Vertical TEC data from TOPEX are believed to be accurate to the 2-3 TECU level (Imel 1994), and is a valuable resource for evaluating GIM TEC map accuracy, especially for ocean altimetry applications.

"Quick-look" TOPEX data are typically available in 8 hour segments within about 8 hours of real time. We can therefore use TOPEX TEC data in our daily process for comparison against the GIM solution and validate our product before delivery. ("Quick-look" TOPEX data are not always available in real-time, due to data flow problems or when the single-frequency SSALT altimeter on board TOPEX/Poseidon is in use. Quick-look TOPEX data are currently typically available about 80% of days, although often only as a partial data set. Also, TOPEX TEC data are only available over bodies of water.) In our GIM-TOPEX comparisons, we compress the TOPEX data to a data rate of 1 point per 12 seconds (to reduce noise) and treat it as truth data. Previous comparisons of TOPEX data with GIM products and climatological models have found that the GIM product is

considerably more accurate than TEC derived from climatological models (Yuan et al 1995).

Fig. 4a shows a plot of GIM TEC, TOPEX TEC and IRI-95 climatological model TEC along the TOPEX/Poseidon track for 6 July 1998. Fig. 4b shows a similar plot for 4 May 1998 on which there was a large ionospheric storm. These days were chosen because the data were relatively unaffected by the Turborogue GPS Receiver L2 tracking problem described below. Also the orientation of the TOPEX/Poseidon orbital plane relative to the sun was roughly the same on these two days. These two days will be discussed in more detail below.

Fig. 5 shows results from comparisons of GIM with TOPEX TEC for days 91 to 330 of 1998. Daily RMS differences between GIM and TOPEX TEC data are displayed for both the 24 hour and 72 hour products. As expected, the 72 hour GIM product is typically better than the 24 hour product since it has the advantage of additional GPS data not available for the 24 hour product. The primary features of the plot are (1) the RMS difference generally varies fairly smoothly during this period from 5.5 to 3 TECU and then back up again, but has occasional sharp peaks, and (2) there is a steady degradation in performance from day of year (DOY) 220 to the end of the comparison data set. (Although not shown, the performance improved after this comparison period.)

The sharp peaks in Fig. 5 are highly correlated with geomagnetic storm activity as indicated by the Ap geomagnetic activity index (Fig. 6). During these periods the ionosphere is highly disturbed, and GIM is less able to track the variation, especially in areas where GPS data coverage is poor and thus must rely on spatial/temporal interpolation or extrapolation (Ho et al 1997). Furthermore, the receiver problems described in the next paragraph also contribute.

The gradual loss of accuracy following DOY 220 (and also some of the peaks and the period before DOY 130) is believed to be largely due to problems in GPS receiver performance. The Turborogue GPS receivers, which are the most common type of

receiver in the IGS network, have a software problem which severely degrades the tracking of the L2 signal when P2-P1 exceeds about 12 m (Zumberge 1998) which corresponds to a line-of-sight TEC of 114 TECU. At low elevation, the obliquity function can reach 3, and the 114 TECU limit thus corresponds to a vertical TEC limit of 40 TECU at low elevation. Since GIM currently relies on dual-frequency data to measure the ionosphere, this seriously limits the data available. As the TEC level rose between DOY 220 and 330, this problem became gradually more severe, especially in the equatorial regions during the daytime where the TEC typically peaks. A rather severe example of receiver performance degradation is shown in Fig. 7 which shows the data volume (after editing) from the Turborogue GPS receiver ASC1 at Ascension Island from days 112 to 326 in 1998. The nighttime data volume is fairly constant over this period, but the noontime data volume drops to zero from day 266 to 326, the end of the period examined. ASC1 is especially susceptible to the Turborogue problem since it is near the magnetic equator and has a large hardware L1/L2 group delay bias.

This high-TEC tracking problem in the receiver software was apparently not noticed in the previous years of the global GPS network, and was first noticed in 1998, due to the rise in global TEC level associated with the approach to the maximum of the solar cycle in the year 2000-2001. The problem with the equatorial GPS receivers will be solved either by fixing the receiver software or substituting receivers. However, we are also working within GIM to resolve the problem. We are currently implementing a single-frequency GPS TEC data type into GIM called DRVID (differenced range vs. integrated doppler), which is essentially the difference between P1 and L1:

$$P1 - L1 = (0.325 \text{ m / TECU}) STEC + B_{\phi}$$

where B_ϕ is an arbitrary phase bias due to the phase cycle ambiguity of the L1 observable. This should help fill the gaps in data coverage caused by the Turborogue L2 problem for past data, and also in the future if the problem persists.

Fig. 4a shows a plot of GIM TEC, TOPEX TEC, and IRI-95 climatological model TEC along the TOPEX/Poseidon track for 6 July 1998. (See also Fig. 2.) As mentioned earlier, this day was chosen because it was relatively unaffected by the Turborogue L2 problem. Evidently, GIM tracks TOPEX TEC considerably more faithfully than IRI-95 does. Table 1 lists the RMS discrepancy between GIM and TOPEX TEC, and between IRI-95 and TOPEX TEC broken down into 5 magnetic latitude bins. The overall RMS discrepancy for the day is 3.7 TECU for GIM and 6.8 TECU for IRI-95. Clearly the largest discrepancy between TOPEX and GIM occurs when TOPEX has a sharp double peak around 5 UT and exceeds GIM by 23 TECU. (The IRI-95 solar/ionosphere coefficients file used in this and the following comparison is the 15 March 1999 version, and may be slightly better than the version available in real time.)

Fig. 4b shows similar data for 4 May 1998 on which there was a strong ionospheric disturbance. This day was also chosen because data loss due to the Turborogue L2 problem was relatively mild on this day, although it still had a deleterious effect on GIM accuracy. GIM's technique of spatial/temporal interpolation using persistence of the TEC structure in the solar-magnetic frame and climatological gradient data leads to larger errors when the ionosphere has so much spatial/temporal volatility and complexity. This problem is most severe in regions where data coverage is sparse, particularly in the low latitude regions. Even so, GIM clearly performed better than IRI-95. There is a large 120 TECU peak in the TEC measured by TOPEX associated with the storm which is not captured by GIM. The TOPEX peak occurs at 5:42 UT at latitude -11 and longitude 105 degrees. There were no GPS receivers within 15 degrees of the peak used in the GIM run (although the Cocos Island GPS receiver is there now). Also, the large TEC at the peak could not be tracked by GPS receivers with the Turborogue L2

problem, since they cannot record L2 data when the slant TEC (plus hardware biases) exceeds 114 TECU. The RMS discrepancies between TOPEX TEC and GIM and IRI-95 are listed in Table 1. The overall RMS discrepancy was 6.67 TECU for GIM and 9.04 TECU for IRI-95.

GIM-TOPEX TEC comparison summary statistics for the entire period from April to December 1998 are listed in Table 2. In this table, TOPEX data for the period were binned by magnetic latitude and local time, and statistics for the difference with GIM TEC (mean, RMS, and standard deviation about the mean) are listed. Only “Quick-look” TOPEX data were used in this comparison. GIM performs best at mid-to-high latitudes, and more poorly at low latitudes. Contributing to this loss of accuracy at low latitude are the problems described above: the relative scarcity of low latitude GPS receivers, the Turborogue L2 problem, errors in the mapping function and shell approximation at low latitudes, and the relative spatial/temporal complexity of the low latitude ionosphere. Another significant feature in the statistics is that the night-time (21 to 3 hours) GIM TEC seems biased too low at all latitudes. This may be due to the use of a uniform shell height globally in our ionospheric model: The centroid height of the electron density of the ionosphere is higher at night than during the day, and use of a higher shell height would be expected to increase the level of the vertical TEC solution extracted by GIM.

5. Ionospheric calibration for ocean altimeters

GIM nominally computes the vertical TEC up to the GPS satellite altitude of 20200 km. The GFO and ERS-2 satellites both carry single-frequency radar altimetry instruments and orbit at an altitude of about 800 km. In order to provide GIM-based ionospheric calibrations for those altimeters, the part of the vertical TEC above 800 km must be subtracted from the GIM TEC. Currently our principal resource for computing the super-satellite TEC comes from climatological model electron density profiles.

We have chosen the IRI-95 model (Bilitza et al 1998) as our model of ionospheric electron density. IRI-95 models the electron density below 1000 km and permits extrapolation of the model above 1000 km. However the extrapolated electron density seems excessively large between 1000 and 2000 km. A standard model of electron density at very high altitudes ($> \sim 1500$ km) is the Gallagher Plasmasphere Model of 1988 (Gallagher et al 1988) which is a static model (i.e. not dependent on season or solar activity or other parameters, unlike the IRI-95 model which can take many input parameters) of the plasmaspheric electron density based on in situ measurements of hydrogen ion density. We tested various combinations of the two models against TEC data from the ERS-2 PRARE instrument, and the ALEXIS and GPSMET satellites, all of which are around 800 km altitude. The results of the comparisons were inconclusive, in part due to possible problems with instrumental biases and slant-to-vertical TEC mapping and other problems in the 800 km satellite data types, but also due to the fact that the results of the candidate super-satellite TEC removal techniques were often not sufficiently different to choose one technique over another. In particular, since the differences among the candidate techniques were so much smaller than the observed GIM-TOPEX discrepancies, implementation of GIM improvements seems a higher priority than improving the super-satellite TEC technique for current development.

Currently we are using the following formula to compute TEC below the altimeter:

$$TEC_{< 800 \text{ km}}(t, \lambda, \phi) = TEC_{GIM}(t, \lambda, \phi) \frac{TEC_{IRI95 < 800 \text{ km}}(t, \lambda, \phi)}{TEC_{IRI95 < 1400 \text{ km}}(t, \lambda, \phi)}$$

where $TEC_{< 800 \text{ km}}(t, \lambda, \phi)$ is the altimeter ionospheric calibration along the satellite ground track at time t , latitude λ , and longitude ϕ , $TEC_{GIM}(t, \lambda, \phi)$ is the GIM TEC at the same place and time, and $TEC_{IRI95 < 800 \text{ km}}(t, \lambda, \phi)$ and $TEC_{IRI95 < 1400 \text{ km}}(t, \lambda, \phi)$ are the TECs below 800 km and 1400 km derived from the IRI-95 climatological model.

Our current technique is a compromise among various considerations: (1) Multiplying the GIM TEC by a fraction based on climatological TEC values to compute sub-satellite TEC is safer than subtracting the climatological model super-satellite TEC from GIM, avoiding such problem situations as when the model super-satellite TEC is larger than the GIM TEC. By using the IRI-95 fraction we rely on what should be hopefully a more reliable fraction of two IRI-95 model quantities, instead of the absolute values. (2) Combining the Gallagher model with IRI-95 can be dangerous, because they are not entirely compatible: The Gallagher model often peaks where IRI-95 has a valley, causing the ratio of the TEC above 800 to the TEC below to be excessively high. Also the IRI-95 model increases and decreases according to the month and solar activity whereas the Gallagher model does not. (3) The IRI-95 electron density model, which is only designed to handle altitudes below 1000 km, is nearly constant as a function of altitude above 1000 km and seems excessively large above 1000 km and so the integral of the density must be cut off at some altitude.

6. Planned improvements

Our primary efforts over the next year will be to improve GIM accuracy by including new data types and improving the filter model. Implementation of GPS L1 DRVID data in GIM is expected to largely fill the data gaps caused by the Turborogue L2 problem. Implementation of TOPEX TEC data in GIM will improve data coverage over the oceans, and ingesting data from GPS occultation satellites is also planned. We are also studying the use of other ionosphere models in GIM (3 dimensional models and more sophisticated shell models) and we will be tuning and testing these new strategies.

7. Conclusions

GIM is a valuable resource providing timely global ionospheric TEC maps, which are being applied to calibrating single-frequency radar ocean altimeter data and also in TOPEX/Poseidon orbit determination. The daily RMS accuracy of GIM TEC maps (based on comparisons with data from the TOPEX altimeter) has been better than 10 TECU (which is 2.2 cm at Ku band, the GFO altimeter frequency) except for a few days in November 1998. Accuracy has been better than 5 TECU in months where the TEC was low. The loss of accuracy during the November period and the lower accuracy in months when the TEC is high, is due at least in part to significant loss of dual-frequency data from software problems in some GPS receivers. These problems are currently being addressed, both by resolving the GPS receiver problems, and by adding single-frequency GPS and other data types to GIM processing. We expect that when the problem with the receivers is corrected, RMS accuracy will typically be better than 5 TECU in the mid-to-high latitudes, and better than 10 TECU in the equatorial region.

Acknowledgements

The research described in this paper was carried out by the Jet Propulsion Laboratory, California Institute of Technology, and was sponsored by the U.S. Naval Oceanographic Office and the National Aeronautics and Space Administration.

References

- Bierman, G.J., 1977. Factorization Methods for Discrete Sequential Estimation, New York, Academic Press.
- Bilitza, D., Rawer, K., Pallaschke, S., 1988. "Study Of Ionospheric Models For Satellite Orbit Determination," Radio Science, 23, 3, pp. 223-232.

Bilitza, D. Rawer, K., 1998. "International Reference Ionosphere Model (IRI-95)," http://envnet.gsfc.nasa.gov/Models/EnviroNET_Models.html.

Coco, D.S., Coker, C., Dahlke, S.R., Clynych, J.R., 1991, "Variability of GPS Satellite Differential Group Delay Biases," IEEE Transactions on Aerospace and Electronic Systems, 27, pp. 931-938.

Gallagher, D.L., Craven, P.D., Comfort, R.H., 1988. "An Empirical Model Of The Earth's Plasmasphere," Advances in Space Research, 8, 8, pp. 15-24.

Ho, C.M., Wilson, B.D., Mannucci, A.J., Lindqwister, U.J., Yuan, D.N., 1997. "A Comparative Study Of Ionospheric TEC Measurements And Models With TOPEX," Radio Science, 32, 4, pp. 1499-1512.

Imel, D.A., 1994, "Evaluation Of The Topex/Poseidon Dual-Frequency Ionosphere Correction," *Journal of Geophysical Research* O, **99**, C12, pp. 24895-24906.

Komjathy, A., 1999. "Comparison and validation of different techniques to provide ionospheric delay corrections for single frequency altimeter measurements", Proceedings of GPS Applications to the Structure and Dynamics of the Earth's Oceans and Ionosphere Workshop, in this issue.

Lanyi, G.E., Roth, T., 1988. "A Comparison Of Mapped And Measured Total Ionospheric Electron Content Using Global Positioning System And Beacon Satellite Observations," Radio Science, 23, pp. 483-492.

Lawson, C., 1984. "A Piecewise C2 Basis for Function Representation over the Surface of a Sphere", JPL internal document.

Lillibridge, J., 1998. Private communication.

Lichten, S.M., 1990. "Estimation and filtering for high precision GPS positioning applications, Manuscr. Geod., 15, 159.

Llewellyn, S.K., Bent, R.B., 1973. Documentation and description of the Bent ionospheric model, Rep. AFCTRL-TR-73-0657, Air Force Geophys. Lab., Hanscom Air Force Base, Mass.

Lough, M.F., Vigue-Rodi, Y., Muellerschoen, R., Haines, B.J., 1998. Private communication.

Mannucci, A.J., Wilson, B.D., Yuan, D.N., Ho, C.M., Lindqwister, U.J., Runge, T.F., 1998. "A Global Mapping Technique For GPS-Derived Ionospheric Total Electron-Content Measurements," Radio Science, 33, 3, pp. 565-582.

Sardon, E., Zarroa, N., 1997, "Estimation Of Total Electron-Content Using GPS Data - How Stable Are The Differential Satellite And Receiver Instrumental Biases," Radio Science, 32, pp. 1899-1910.

Schaer, S., Gurtner, W., Feltens, J., 1998. "IONEX: The IONosphere Map EXchange Format Version 1," <ftp://igs.cb.jpl.nasa.gov/igs.cb/data/format/ionex1.ps> .

Vladimer, J.A., Lee, M.C., Doherty, P.H., Decker, D.T., Anderson, D.N., 1997, "Comparisons of Topex and Global Positioning System Total Electron-Content Measurements at Equatorial Anomaly Latitudes," *Radio Science*, 32, 6, pp. 2209-2220.

Wilson, B.D., Mannucci, A.J., 1994, "Extracting Ionospheric Measurements From GPS In The Presence Of Anti-Spoofing," in *Proceedings of the Seventh International Technical Meeting of the Satellite Division of the Institute of Navigation ION-GPS 94*, (available from the Institute of Navigation, 1800 Diagonal Road, Suite 480, Alexandria, VA), pp. 1599-1608.

Wilson, B.D., Mannucci, A.J., Edwards, C.D., 1995. "Subdaily Northern-Hemisphere Maps Using An Extensive Network Of GPS Receivers," *Radio Science*, 30, 3, pp. 639-648.

Yuan, D.N., Mannucci, A.J., Wilson, B.D., Runge, T.F., Lindqwister, U.J., 1995. "Shell Height And Vertical TEC Mapping Function Analysis For Ionospheric Shell Model," *EOS Transactions of the AGU*, 76, 17, Spring Meeting Supplement (available from American Geophysical Union, 2000 Florida Avenue, NW, Washington DC 20009), pp. S87.

Zumberge, J.F., Liu, R., Neilan, R.E., (Eds.), 1994. *International GPS Service for Geodynamics 1994 Annual Report*, JPL Publ. 95-18, p. 329.

Zumberge, J.F., 1998. Private communication.

Tables

Table 1. Daily RMS discrepancy between GIM and TOPEX TEC, and between IRI-95 and TOPEX for 6 Jul 1998 and 4 May 1998 as function of absolute value of magnetic latitude (in degrees). Units for TEC discrepancies are TECU.

	6 Jul		4 May	
Magnetic Latitude	GIM	IRI-95	GIM	IRI-95
0-20	4.7	7.9	7.7	10.7
20-30	3.2	7.1	10.7	12.8
30-40	3.2	7.3	5.0	9.2
40-55	2.7	5.5	4.0	5.8
55-90	3.9	5.2	6.0	6.1
Global	3.7	6.8	6.7	9.0

Table 2. Summary of GIM minus TOPEX TEC statistics for Apr-Dec 1998. Data are binned by absolute magnetic latitude and local time. The first two columns list the magnetic latitude range (degrees), the next two columns list the local time range (hours past midnight). The next column is the number of data available for that bin, and the next three columns are the mean, standard deviation and RMS values for GIM minus TOPEX TEC in TECU. After the statistics binned by magnetic latitude and local time, statistics binned by magnetic latitude alone and by local time alone are listed. The final line lists global statistics.

Magnetic	Local	Number	Diff	Diff	Diff
latitude	time	data	Mean	Std Dev	RMS

0	20	3	9	49869	-1.69	3.42	3.82
		9	15	51789	-0.46	7.34	7.36
		15	21	51273	-1.23	8.94	9.03
		21	3	50537	-3.09	6.99	7.64
20	30	3	9	25192	-0.86	3.21	3.33
		9	15	27568	1.46	6.22	6.39
		15	21	26537	0.36	6.34	6.35
		21	3	27764	-1.91	4.19	4.60
30	40	3	9	26720	-1.30	3.01	3.28
		9	15	29334	1.31	3.82	4.04
		15	21	28685	0.27	3.35	3.36
		21	3	30582	-2.34	2.84	3.68
40	55	3	9	43671	-1.90	3.12	3.65
		9	15	45347	-0.16	3.01	3.01
		15	21	49310	-1.37	3.31	3.58
		21	3	51481	-3.61	4.15	5.51
55	90	3	9	29546	-3.00	2.63	3.98
		9	15	30296	-1.57	3.04	3.42
		15	21	35909	-2.45	3.48	4.26
		21	3	35129	-3.97	3.69	5.42
0	20	0	24	203468	-1.61	7.06	7.24
20	30			107061	-0.23	5.34	5.35
30	40			115321	-0.52	3.57	3.61
40	55			189809	-1.81	3.68	4.10
55	90			130880	-2.78	3.38	4.38
0	90	3	9	174998	-1.78	3.20	3.66
		9	15	184334	0.00	5.30	5.30
		15	21	191714	-1.05	5.89	5.98
		21	3	195493	-3.10	4.89	5.79

0 90 0 24 746539 -1.50 5.08 5.29

Figure captions

Fig. 1. GPS global network. Triangles indicate locations of GPS receivers of the IGS and other organizations. Circles around the triangles indicate the portion of the ionosphere visible from the site assuming an ionospheric shell height of 450 km and an elevation cutoff of 10 degrees.

Fig. 2. GIM vertical TEC map for 6 July 1998 17 UT. The horizontal plot axis is "local time," for example the ionospheric vertical TEC peaked near 2 pm north of Brazil. The dots indicate the locations of the GPS receivers processed by GIM this day.

Fig. 3. Daily GIM process data flow. The process is run on an HP 9000/780 platform. The GPS data are imported from other JPL computers and IGS data centers. TOPEX data and GFO and ERS-2 ephemerides are also imported. Data are processed to produce global TEC maps, GPS receiver and satellite hardware biases, and altimeter calibration files, which are exported to users.

Fig. 4a. TOPEX TEC for 6 July 1998, and the GIM and IRI-95 TEC calibrations along the TOPEX/Poseidon ground track. TOPEX data is only available when the TOPEX/Poseidon satellite is over water. This day was chosen as an example of a day the ionosphere was fairly quiet and Turborogue L2 problem was quite mild. (See Figs. 4b and 4c for a day when GIM performed less well due to an ionospheric storm.) GIM clearly tracks TOPEX much more faithfully than IRI-95.

Fig. 4b. TOPEX TEC for 4 May 1998, and the GIM and IRI-95 TEC calibrations along the TOPEX/Poseidon ground track. This day was chosen as an example of a day when there was a very large ionospheric disturbance causing GIM to perform less well. This day was also chosen because data loss due to the Turborogue L2 problem was relatively mild on this day. Even so, it still had a deleterious effect on GIM accuracy. GIM clearly performed better than IRI-95.

Fig. 4c. This is a detail from Fig. 4b showing the TOPEX TEC data at the peak of the effect of the ionospheric storm.

Fig. 5. GIM-TOPEX comparisons for days 91 to 330 of 1998. Plotted are the daily RMS difference between GIM TEC and TOPEX TEC along the TOPEX/Poseidon ground track. Both the results for the 24 hour and 72 hour-latency GIM runs are plotted. Sharp peaks in the geomagnetic activity index, A_p , are associated with sharp peaks in the RMS difference. (See also Fig. 6.)

Fig. 6. The geomagnetic activity index “ A_p ” is plotted versus day for days 100 to 321 of 1998. Sharp peaks in A_p on days 124, 239, 268, 312, and 317 are highly correlated with sharp peaks in GIM-TOPEX comparisons of Fig. 5.

Fig. 7. GPS data volume (after editing) for the Turborogue GPS receiver on Ascension Island near local noon (12-15 local time) and local midnight (0-3) for days 112 to 326. The noontime data volume dropped to zero after day 260 due to high TEC and the Turborogue L2 bug.

Figures

Fig. 1 follows

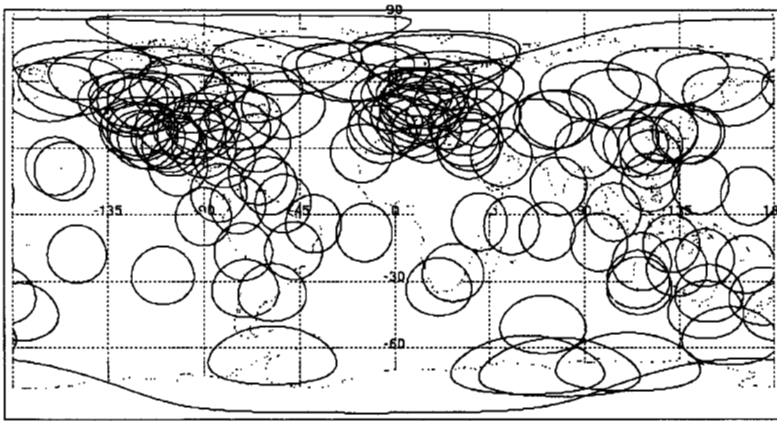


Fig. 2 follows

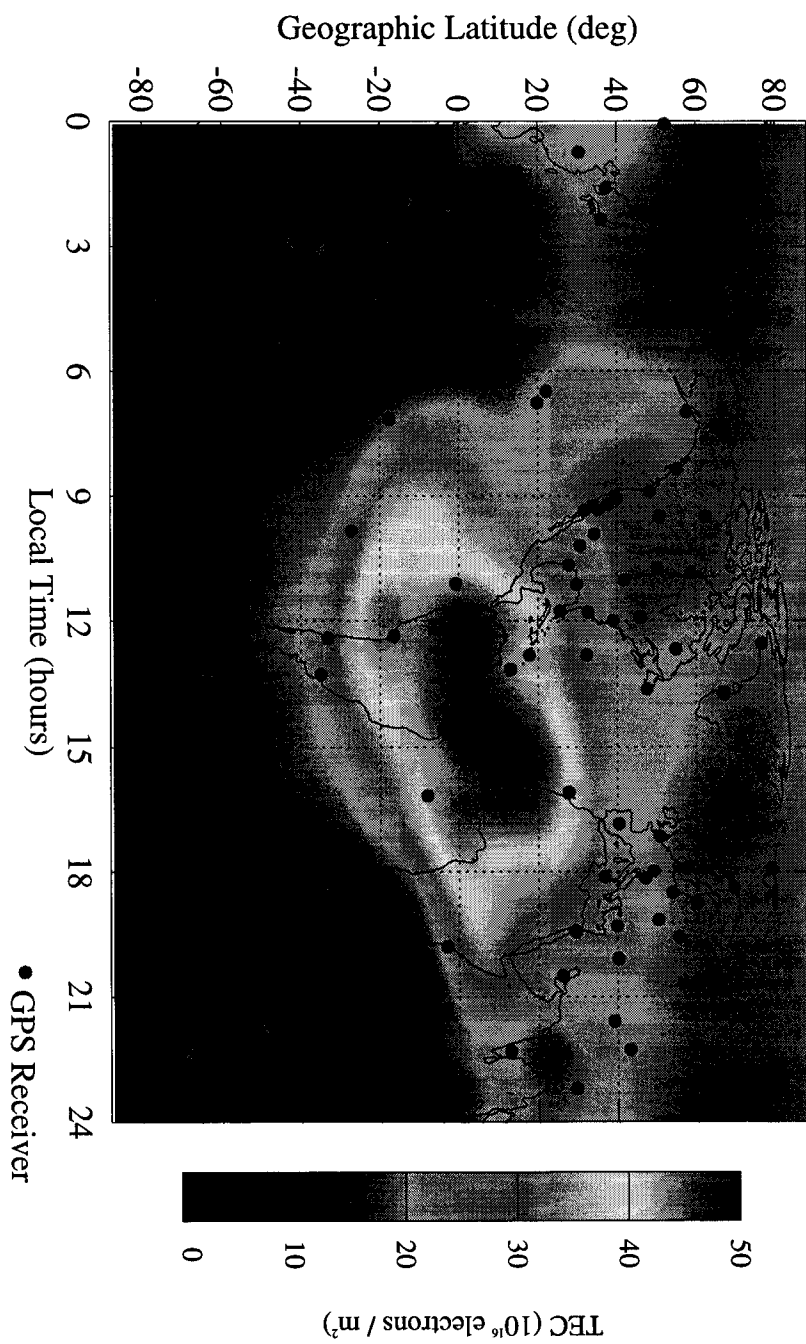


Fig. 3 follows

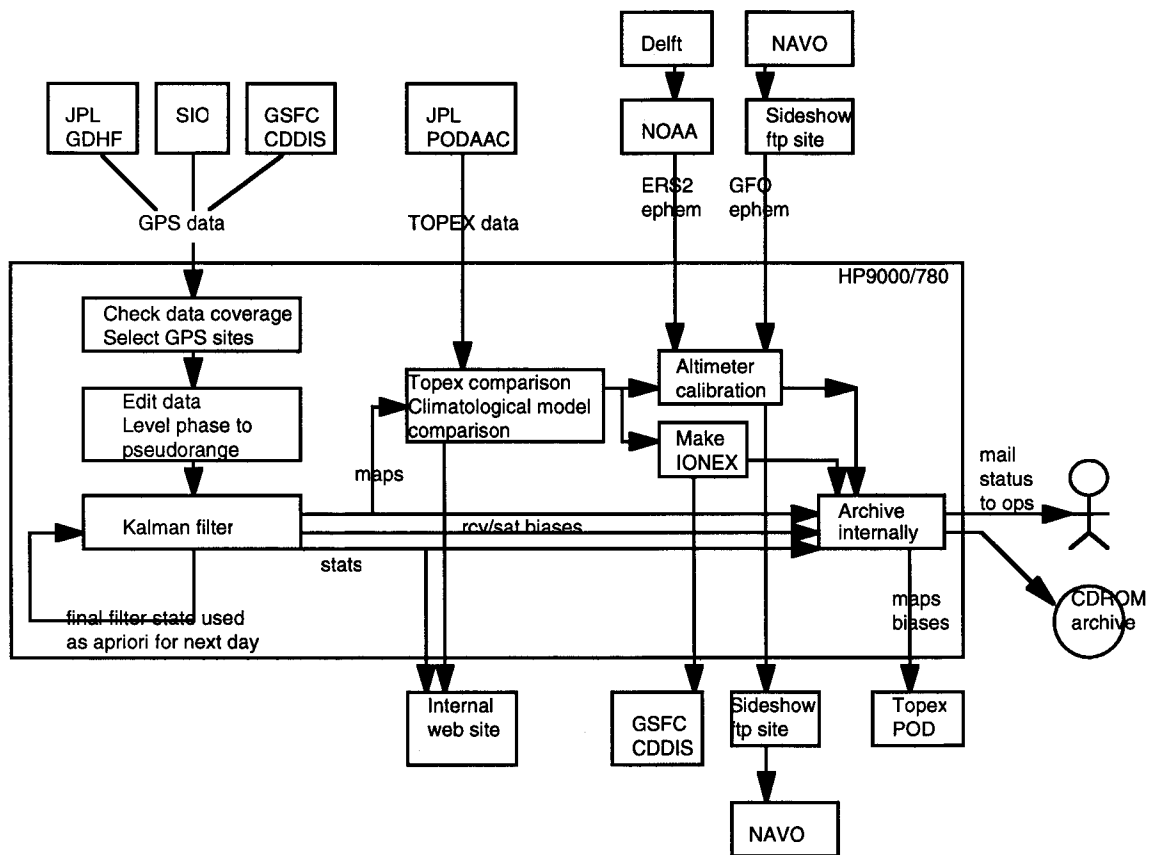
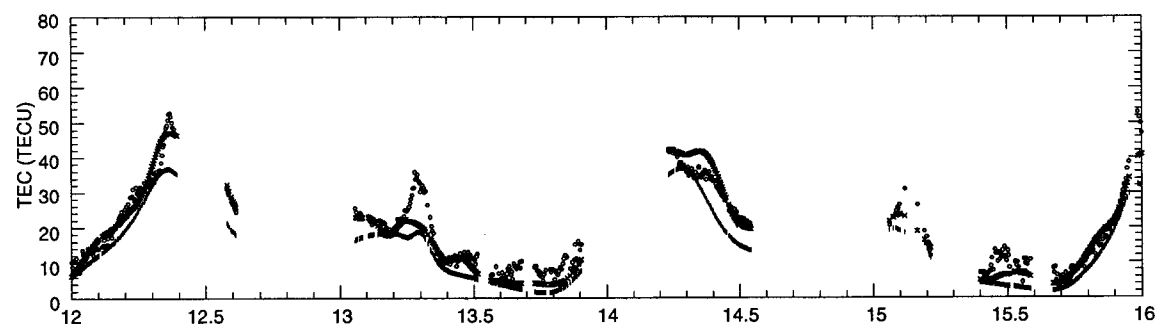
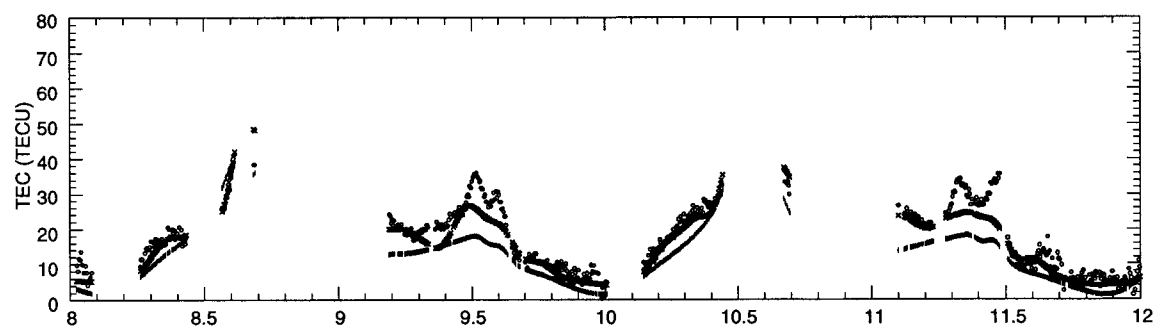
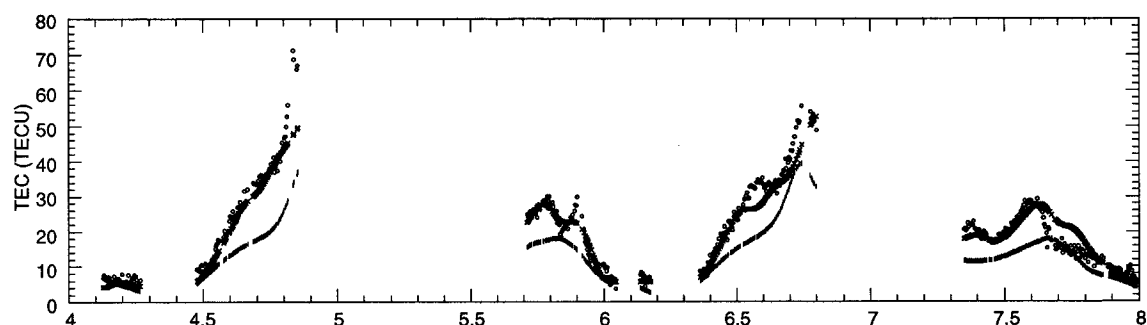
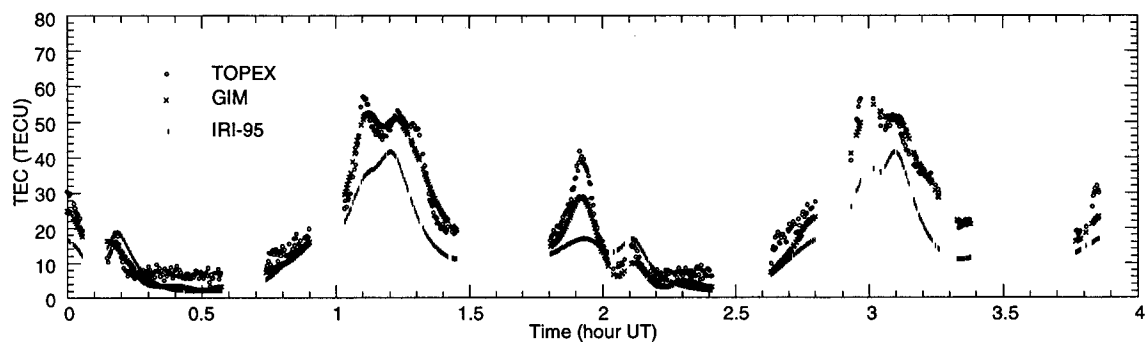


Fig. 4a follows



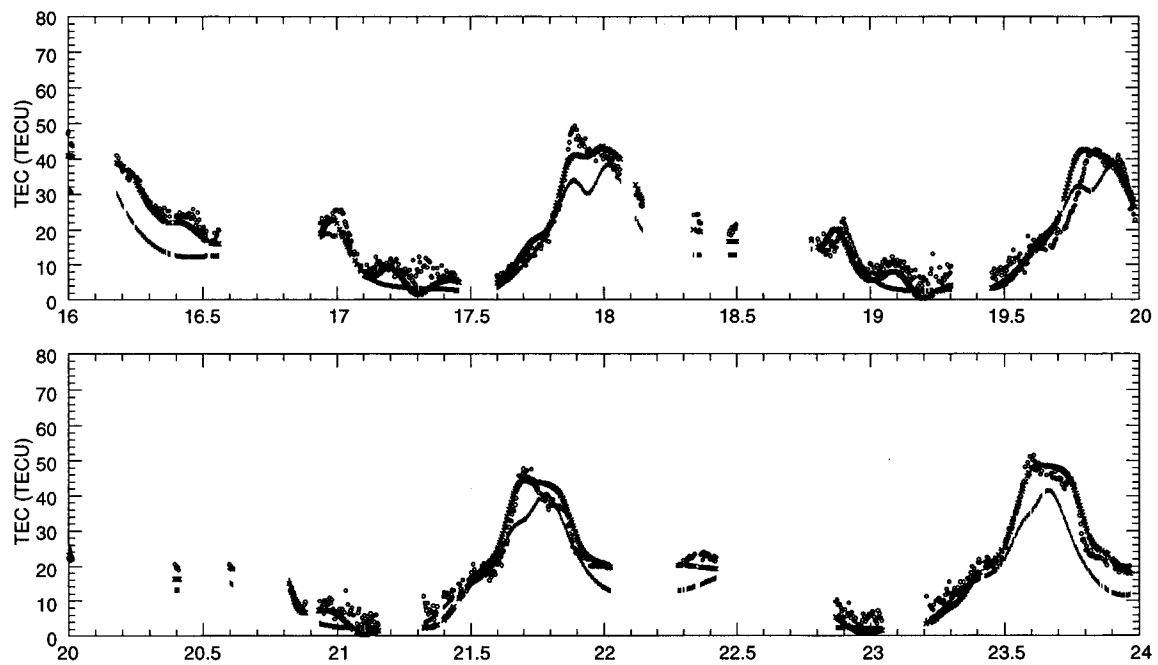
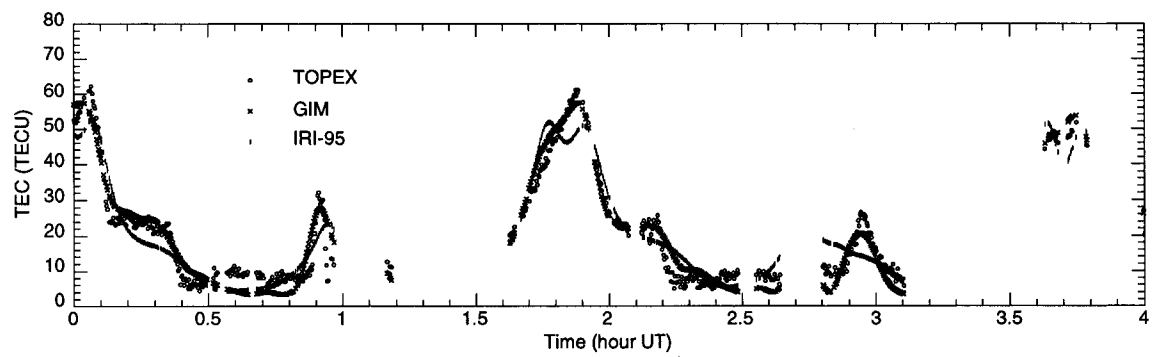


Fig. 4b follows



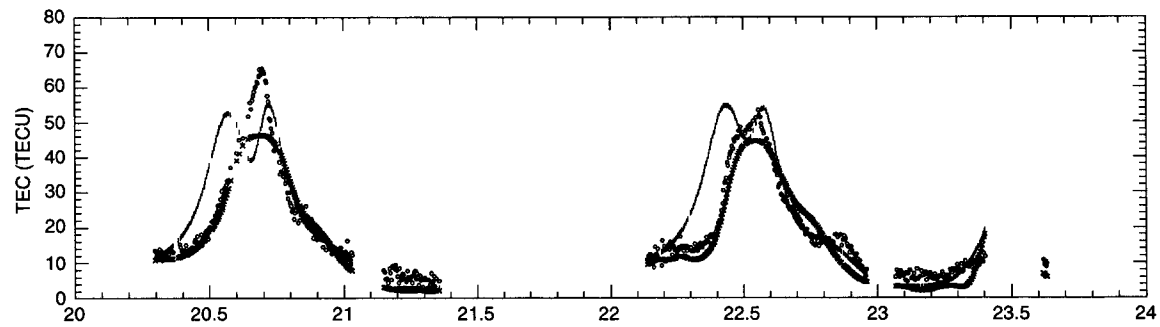
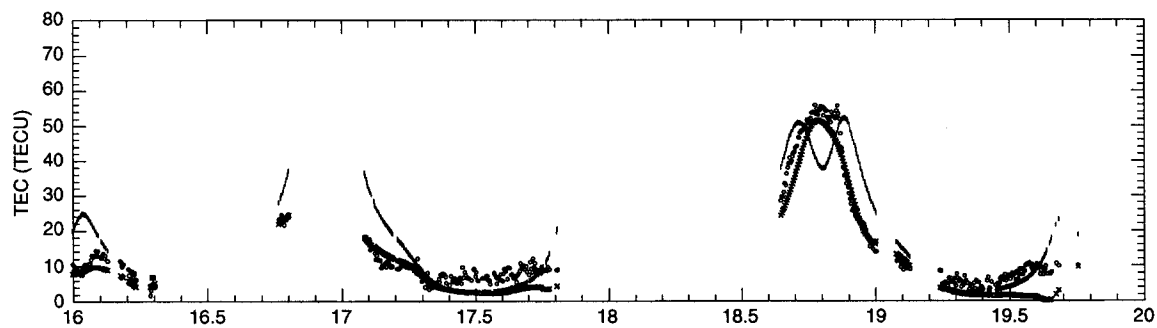
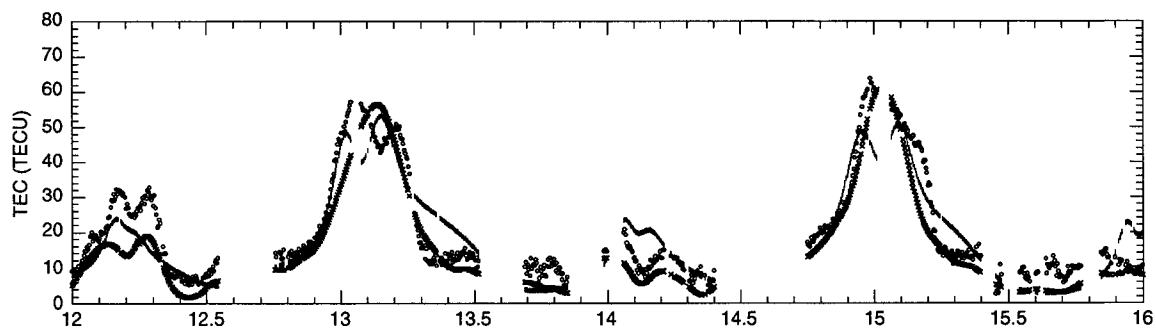
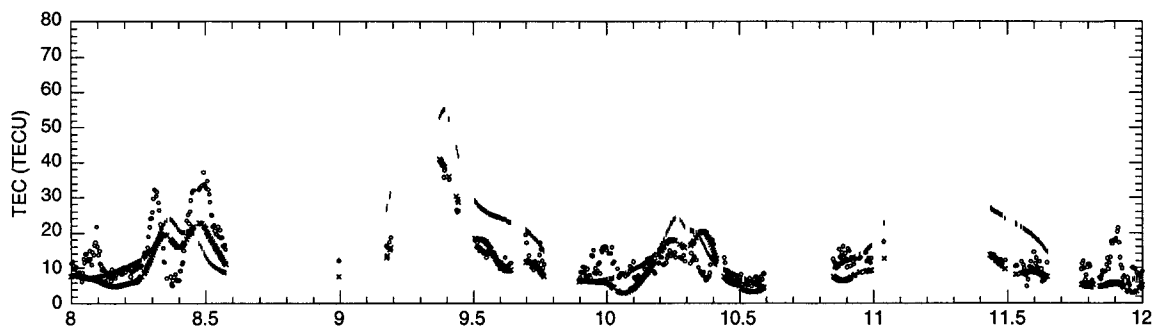
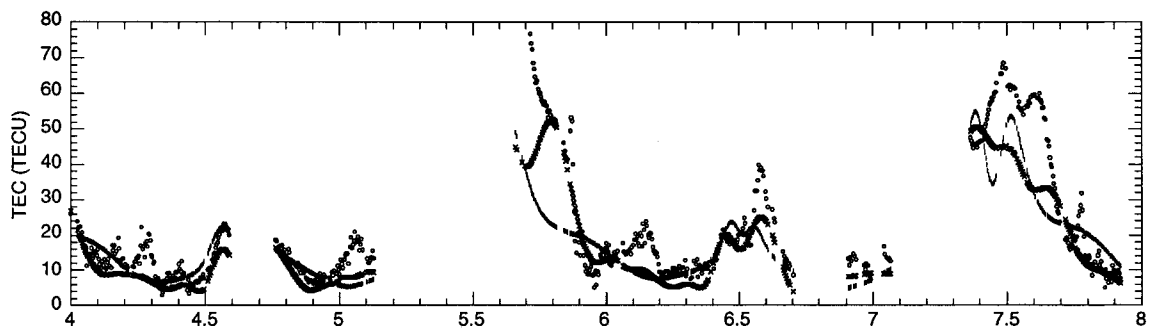


Fig. 4c follows

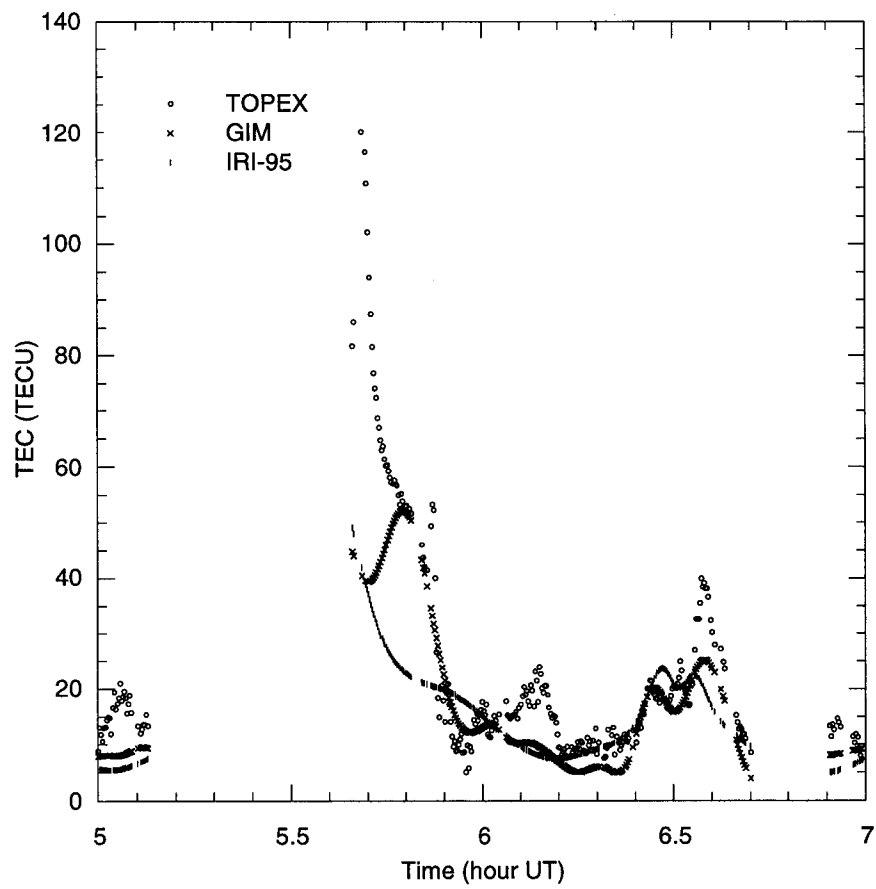


Fig. 5 follows

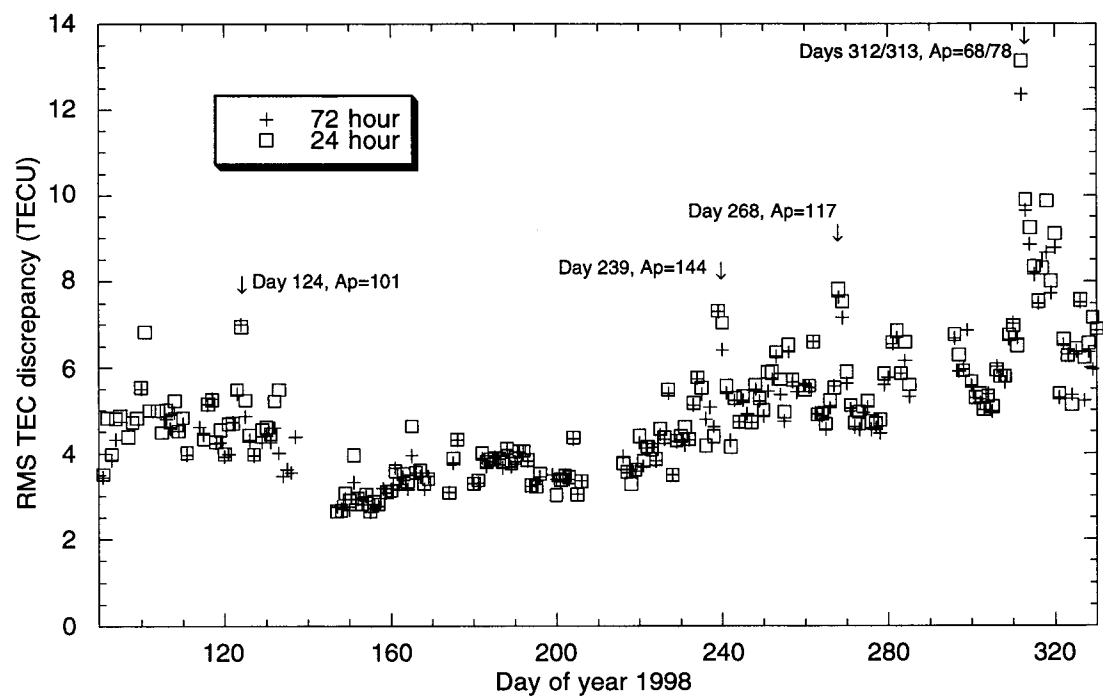


Fig. 6 follows

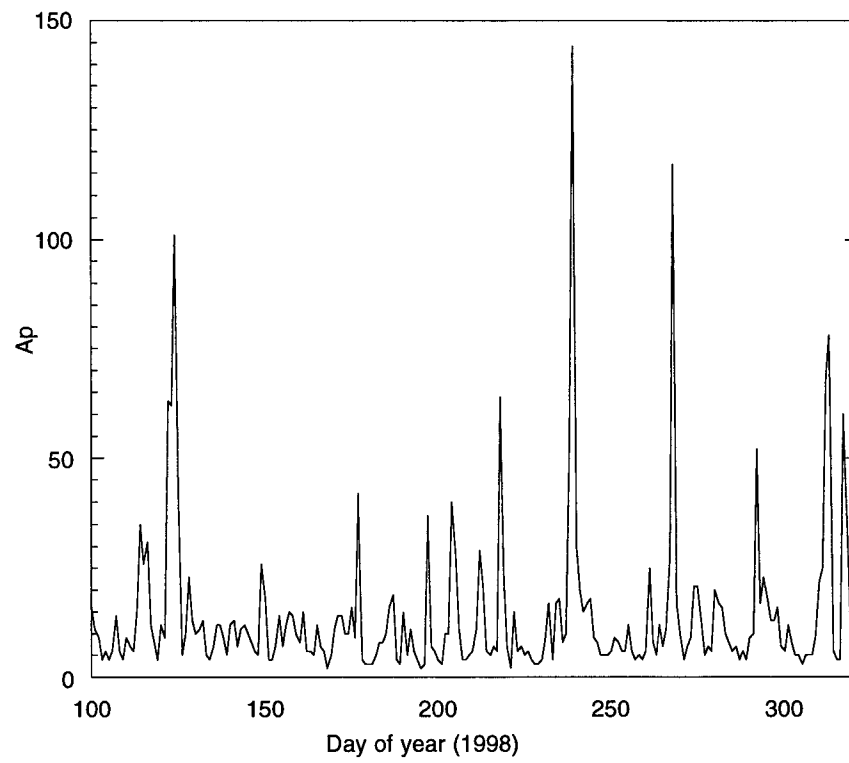


Fig. 7 follows

